

Cite this: *Chem. Sci.*, 2023, 14, 10524

All publication charges for this article have been paid for by the Royal Society of Chemistry

Direct conversion of amino acids to oxetanol bioisosteres via photoredox catalysis†

Avelyn Mae V. Delos Reyes,^{ID} ^{ac} Christopher S. Nieves Escobar,^{ID} ^{bc} Alberto Muñoz,^c Maya I. Huffman^{ID} ^{cd} and Derek S. Tan^{ID} ^{*abcde}

Carboxylic acids are an important structural feature in many drugs, but are associated with a number of unfavorable pharmacological properties. To address this problem, carboxylic acids can be replaced with bioisosteric mimics that interact similarly with biological targets but avoid these liabilities. Recently, 3-oxetanols have been identified as useful carboxylic acid bioisosteres that maintain similar hydrogen-bonding capacity while decreasing acidity and increasing lipophilicity. However, the installation of 3-oxetanols generally requires multistep *de novo* synthesis, presenting an obstacle to investigation of these promising bioisosteres. Herein, we report a new synthetic approach involving direct conversion of carboxylic acids to 3-oxetanols using a photoredox-catalyzed decarboxylative addition to 3-oxetanone. Two versions of the transformation have been developed, in the presence or absence of CrCl₃ and TMSCl cocatalysts. The reactions are effective for a variety of *N*-aryl α -amino acids and have excellent functional group tolerance. The Cr-free conditions generally provide higher yields and avoid the use of chromium reagents. Further, the Cr-free conditions were extended to a series of *N,N*-dialkyl α -amino acid substrates. Mechanistic studies suggest that the Cr-mediated reaction proceeds predominantly *via in situ* formation of an alkyl-Cr intermediate while the Cr-free reaction proceeds largely *via* radical addition to a Brønsted acid-activated ketone. Chain propagation processes provide quantum yields of 5 and 10, respectively.

Received 17th February 2023
Accepted 26th August 2023

DOI: 10.1039/d3sc00936j

rsc.li/chemical-science

Introduction

The carboxylic acid moiety is an important structural feature found in many drugs and other bioactive compounds.¹ However, it is also associated with several pharmacological liabilities, including limited permeability across biological membranes, high plasma protein binding, rapid renal clearance, and conversion to chemically reactive metabolites associated with toxicity.^{2–7} Indeed, small-molecule drugs containing carboxylic acid moieties have been withdrawn from the market at a much higher rate (39%)⁸ than their prevalence would predict (13%).¹ One approach to circumvent undesired

pharmacological properties associated with a given chemical group is to replace it with a bioisostere, a structural mimic that can induce a similar biological response.⁹ Several carboxylic acid bioisosteres have been reported, including hydroxamic acids, phosphonic acids, tetrazoles, and isothiazoles.⁵ Recently, 3-oxetanols have also been identified as promising carboxylic acid bioisosteres that can accommodate similar hydrogen-bonding interactions with biological targets while being less acidic, non-anionic under physiologic conditions, and more lipophilic to provide increased membrane permeability (Fig. 1a).¹⁰ While several synthetic approaches to 3-oxetanols have been reported,^{10–13} they require multistep *de novo* synthesis, presenting an obstacle to broad exploration of this promising class of bioisosteres. In contrast, a method for direct conversion of carboxylic acids to 3-oxetanols would provide expedient access to this motif, facilitating its investigation in medicinal chemistry campaigns. Herein, we report a new synthetic approach that enables direct conversion of α -amino acids to corresponding 3-oxetanols using visible light photoredox-catalyzed decarboxylative addition to 3-oxetanone. The reaction can be carried out in the presence or absence of CrCl₃ and TMSCl cocatalysts, with the Cr-free conditions generally providing higher yields and avoiding the use of chromium reagents. The reactions provide broad substrate scope and functional group compatibility across *N*-aryl α -amino

^aPharmacology Graduate Program, Weill Cornell Graduate School of Medical Sciences, Memorial Sloan Kettering Cancer Center, New York, New York 10065, USA. E-mail: tand@mskcc.org

^bTri-Institutional PhD Program in Chemical Biology, Memorial Sloan Kettering Cancer Center, New York, New York 10065, USA

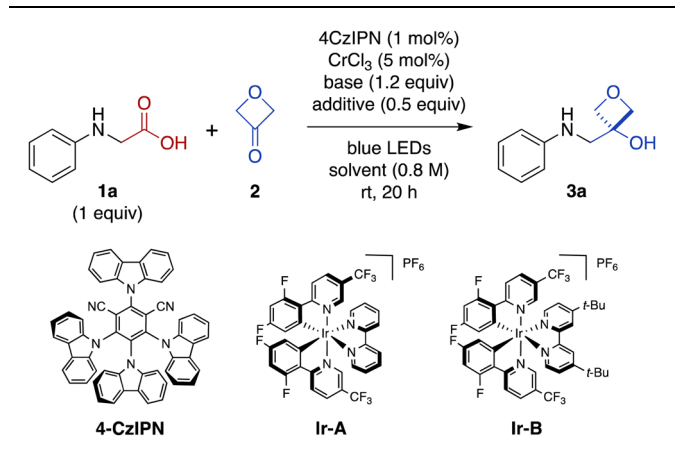
^cChemical Biology Program, Sloan Kettering Institute, Memorial Sloan Kettering Cancer Center, New York, New York 10065, USA

^dTri-Institutional Chemical Biology Summer Program, Memorial Sloan Kettering Cancer Center, New York, New York 10065, USA

^eTri-Institutional Research Program, Memorial Sloan Kettering Cancer Center, New York, New York 10065, USA

† Electronic supplementary information (ESI) available: Experimental procedures and analytical data for all new compounds. See DOI: <https://doi.org/10.1039/d3sc00936j>



Table 1 Discovery and optimization of the carboxylic acid-to-3-oxetanol transformation

Entry	2 (equiv.)	Base	Additive	Solvent	Yield ^a (%)
1	0.5	—	—	DMA	0
2	0.5	CsOAc	—	DMA	7
3	0.5	CsOAc	TMSCl	DMA	22
4	0.5	CsOAc	TMSCl	DMF	25
5 ^b	0.5	CsOAc	TMSCl	DMF	24
6 ^c	0.5	CsOAc	TMSCl	DMF	17
7	0.5	KHCO ₃	TMSCl	DMF	24
8	0.5	CsOPiv	TMSCl	DMF	32
9	0.5	CsOPiv	TMSCl	THF	38
10	0.5	CsOPiv	TMSCl	CH ₃ CN	40
11	0.5	CsOPiv	TESCl	CH ₃ CN	37
12	1.0	CsOPiv	TMSCl	CH ₃ CN	60
13	2.0	CsOPiv	TMSCl	CH ₃ CN	55
14 ^d	1.0	CsOPiv	TMSCl	CH ₃ CN	50
15 ^d	1.0	CsOPiv	—	CH ₃ CN	47
16 ^e	1.0	CsOPiv	TMSCl	CH ₃ CN	0

^a Yields based on ¹H-NMR analysis of crude reaction product in the presence of an internal standard, relative to *N*-phenyl glycine (theoretical maximum 50% for entries 1–11). ^b Photocatalyst: **Ir-A** = [Ir{dF(CF₃)₂ppy}₂(bpy)]PF₆ = [2,2'-bipyridine-*N*1,*N*1']bis[3,5-difluoro-2-[5-(trifluoromethyl)-2-pyridinyl-*N*]phenyl-*C*]iridium(III) hexafluorophosphate. ^c Photocatalyst: **Ir-B** = [Ir{dF(CF₃)₂ppy}₂(dtbpy)]PF₆ = [4,4'-bis(1,1-dimethylethyl)-2,2'-bipyridine-*N*1,*N*1']bis[3,5-difluoro-2-[5-(trifluoromethyl)-2-pyridinyl-*N*]phenyl-*C*]iridium(III) hexafluorophosphate. ^d In absence of CrCl₃. ^e In absence of blue LED light. 4CzIPN = 1,2,3,5-tetrakis(carbazole-9-yl)-4,6-dicyanobenzene, 2,4,5,6-tetrakis(9*H*-carbazol-9-yl) isophthalonitrile; DMA = *N,N*-dimethyl acetamide, DMF = *N,N*-dimethyl formamide; TES = triethylsilyl; THF = tetrahydrofuran; TMS = trimethylsilyl.

In these initial experiments, we used 3-oxetanone as the limiting substrate, by analogy to the conditions reported by Glorius.¹⁵ Next, we investigated alternative stoichiometric ratios (entries 11–13 and ESI Table S1†), and found that the reaction was most effective with equimolar amounts of the two substrates, providing a serviceable 60% yield (entry 12). Interestingly, the reaction also proceeded in the absence of CrCl₃ (Table 1, entry 14), as well as in the absence of both CrCl₃ and TMSCl (entry 15), albeit in lower yields; the mechanistic implications of this finding are discussed below. In contrast, control reactions performed in the absence of light (entry 15) or

photocatalyst (see ESI Table S1†) did not afford any of the desired product.

Substrate scope and functional group tolerance of the Cr-mediated carboxylic acid-to-3-oxetanol transformation

Next, we investigated the scope of the Cr-mediated reaction using other *N*-aryl α -amino acid substrates (Fig. 2). A variety of other substrates were tolerated, including systems derived from alanine (**3b**), leucine (**3c**), phenylalanine (**3d**), tryptophan (**3e**), valine (**3f**) and isoleucine (**3g**). The reaction was also effective in a proline-derived system containing a tertiary amine (**3h**), as well as a corresponding acyclic *N*-methyl alanine-derived system (**3i**) and an indoline-derived system (**3j**). Notably, the reaction also proceeded efficiently with an α,α -dimethylglycine-derived substrate to form 3-oxetanol **3k** having two adjacent quaternary carbons.

A wide range of functional groups were tolerated in other substrates, including a methionine thioether (**3l**), Boc-protected lysine side chain (**3m**), serine benzyl and *t*-butyl ethers (**3n** and **3o**), a tyrosine aryl ether (**3p**), protected aspartate and glutamate esters (**3q** and **3r**), and an asparagine *N*-trityl amide (**3s**). Notably, a free carboxylic acid was also tolerated in an aspartate-derivative system (**3t**), with transformation to the 3-oxetanol occurring regioselectively at the main-chain carboxylate (34%).

We also investigated the influence of electronics of the aromatic ring using a variety of electron-donating and -withdrawing substituents (**3u–x**), but no clear reactivity trends were apparent across this series.

Finally, reaction of a symmetrical diacid substrate **1y** was evaluated in the presence of 2 equiv. 3-oxetanone (**2**) (Fig. 2b). The major product was mono-oxetanol **3z** with protodecarboxylation observed at the second site, while only 10% of the di-oxetanol **3y** was recovered.

Development of Cr-free carboxylic acid-to-3-oxetanol transformation

We were intrigued by the discovery above that the photoredox-catalyzed decarboxylative addition reaction also proceeded effectively in the absence of CrCl₃ and TMSCl (Table 1, entry 14). Thus, we investigated further optimization of this Cr-free reaction using *N*-phenyl valine (**1f**), because the Cr-mediated reaction provided a low yield for this substrate (Figure 2, 28%). Omitting CrCl₃ and TMSCl from the Cr-mediated reaction conditions afforded only a 9% of the desired product (Table 2, entry 1; see ESI Table S2† for complete details). We noted that there was little difference in yield when the reaction time was shortened from 20 h to 2 h (entry 2), facilitating further evaluation of reaction conditions. Investigation of various stoichiometric ratios (entries 2–5) showed that increasing 4CzIPN catalyst loading to 2 mol% and 3-oxetanone to 3 equiv. provided a modest increase in yield to 13%. Evaluation of other solvents (entries 5–8) afforded a dramatic increase in yield in CH₂Cl₂ (89%). Bases other than CsOPiv (entries 9 and 10) and photocatalysts other than 4CzIPN (entries 11 and 12) were far less effective. The reaction also remained dependent upon light (entry 13). We note that König and coworkers have previously



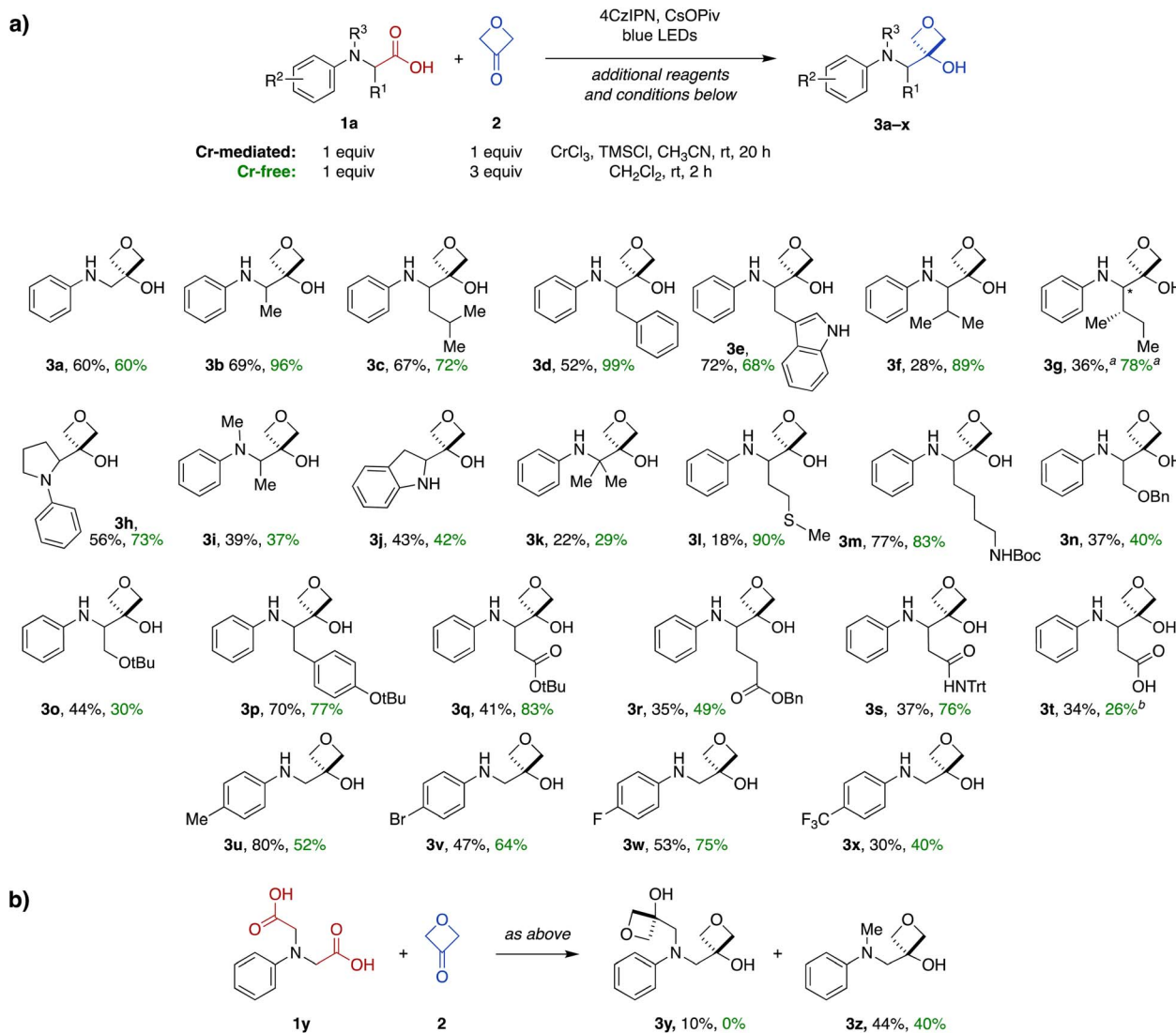


Fig. 2 (a) Scope of the carboxylic acid-to-3-oxetanone transformation for *N*-aryl α -amino acid substrates under Cr-mediated (black yields) and Cr-free reaction conditions (green yields). (b) Conversion of diacid **1y** to mono- (**3y**) and di-oxetanone (**3z**) products. Cr-mediated reaction conditions: 1 mol% 4CzIPN, 5 mol% CrCl₃, 0.5 equiv. TMSCl, 1.2 equiv. CsOPiv, 0.8 M in CH₃CN based on amino acid substrate **1**, blue LED light, rt, 20 h. Cr-free reaction conditions: 2 mol% 4CzIPN, 1.2 equiv. CsOPiv, 0.5 M in CH₂Cl₂ based on amino acid substrate **1**, blue LED light, rt, 2 h. ^adiastereomeric ratio = 1 : 1.4. ^bReaction carried out in isopropanol instead of CH₂Cl₂.

reported photocatalyzed decarboxylative additions of arylacetic acids to aldehydes under similar conditions.¹⁴ However, application of the literature conditions (4CzIPN, Cs₂CO₃, DMA, LED, rt, 16 h) to our substrate **1f** did not afford any of the desired 3-oxetanone product **3f**.

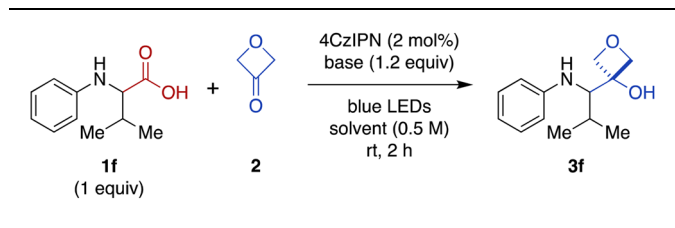
Next, we investigated the substrate scope of the Cr-free reaction across the panel of *N*-aryl α -amino acid substrates (Fig. 2). In most cases, the Cr-free reaction provided higher yields of the 3-oxetanone products compared to those observed with the Cr-mediated reaction, in some cases dramatically so (e.g., **3d**, **3f**, **3g**, **3l**, **3q**, **3s**). Across the entire panel (**3a-x**), the average yield was 64% for the Cr-free reaction compared to 48% for the Cr-mediated reaction. In the case of the diacid substrate **1y**, the Cr-free reaction provided the mono-oxetanone **3z** exclusively. Overall, the Cr-free reaction provides significant advantages over the original Cr-mediated reaction with respect to

efficiency (time, yield) and elimination of toxic and reactive reagents (CrCl₃, TMSCl).

To expand the scope of this transformation beyond *N*-aryl α -amino acid substrates, we investigated Cr-free reactions of other amino acids. In preliminary experiments, we found that exposure of primary (phenylalanine), secondary (*N*-trityl glycine), and *N*-acylated (*N*-Boc-glycine, *N*-Cbz-proline, *N*-phthaloylglycine) α -amino acids to the reaction conditions did not afford any of the desired 3-oxetanone products (not shown). However, morpholine acetic acid was converted to the desired product, albeit with some bis and tris modification observed by MS, presumably at the ring carbons α to the amine. Selectivity for monofunctionalization was improved by decreasing 3-oxetanone stoichiometry from 3 equiv. to 1 equiv. With other slight modifications (changing solvent from CH₂Cl₂ to *i*-PrOH to improve solubility; increasing reaction time to 20 h), the desired



Table 2 Optimization of the Cr-free carboxylic acid-to-3-oxetanol transformation



Entry	2 (equiv.)	Base	Solvent	Yield ^a (%)
1 ^{b,c}	1.0	CsOPiv	CH ₃ CN	9
2 ^b	1.0	CsOPiv	CH ₃ CN	8
3 ^b	2.0	CsOPiv	CH ₃ CN	10
4 ^b	3.0	CsOPiv	CH ₃ CN	11
5	3.0	CsOPiv	CH ₃ CN	13
6	3.0	CsOPiv	DCE	57
7	3.0	CsOPiv	CH ₂ Cl ₂	89
8	3.0	CsOPiv	i-PrOH	78
9	3.0	Na ₂ CO ₃	CH ₂ Cl ₂	24
10	3.0	DIPEA	CH ₂ Cl ₂	21
11 ^d	3.0	CsOPiv	CH ₂ Cl ₂	43
12 ^e	3.0	CsOPiv	CH ₂ Cl ₂	30
13 ^f	3.0	CsOPiv	CH ₂ Cl ₂	0

^a Yields based on ¹H-NMR analysis of crude reaction product in the presence of an internal standard, relative to *N*-phenyl valine (**1f**).

^b 1 mol% 4CzIPN. ^c 20 h reaction time. ^d Photocatalyst: **Ir-A** = [Ir{dF(CF₃)₂ppy}₂(bpy)]PF₆ = [2,2'-bipyridine-*N*,*N*'-bis[3,5-difluoro-2-(5-(trifluoromethyl)-2-pyridinyl-*N*)phenyl-*C*]iridium(III) hexafluorophosphate.

^e Photocatalyst: **Ir-B** = [Ir{dF(CF₃)₂ppy}₂(dtbpy)]PF₆ = [4,4'-bis(1,1-dimethylethyl)-2,2'-bipyridine-*N*,*N*'-bis[3,5-difluoro-2-(5-(trifluoromethyl)-2-pyridinyl-*N*)phenyl-*C*]iridium(III) hexafluorophosphate. ^f In absence of blue LED light. DCE = 1,2-dichloroethane; DIPEA = *N,N*-diisopropylethylamine.

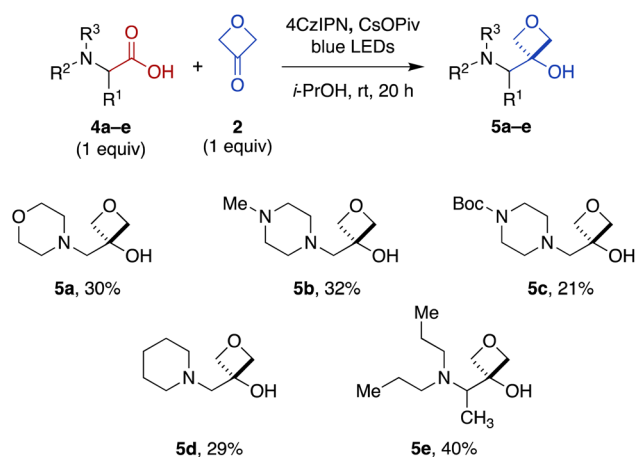


Fig. 3 Direct carboxylic acid-to-3-oxetanol transformation for cyclic and acyclic *N,N*-dialkyl α -amino substrates under modified Cr-free reaction conditions.

3-oxetanol **5a** was obtained in 30% yield (Fig. 3). The reaction was also effective for systems containing *N*-methylpiperazine (**5b**), *N*-Boc-piperazine (**5c**), piperidine (**5d**), and an acyclic

tertiary amine (**5e**), demonstrating tolerance of heteroatoms, protecting groups, and both cyclic and acyclic substrates.

Mechanistic investigations

Next, we probed the mechanisms of the Cr-mediated and Cr-free transformations. We considered three possible mechanisms *a priori*: (1) addition of an α -amino carbanion (or Nozaki-Hiyama-Kishi alkyl-Cr intermediate) to 3-oxetanone,^{15,26} (2) addition of an α -amino radical to 3-oxetanone,³⁹ or (3) radical-radical recombination of an α -amino radical and 3-oxetanone-derived radical.³⁴

First, to assess the reactivity of each of the substrates and reagents to photoactivated 4CzIPN, we conducted fluorescence quenching studies with *N*-phenylglycine (cesium salt) (**1a**), 3-oxetanone (**2**), CsOPiv, TMSCl, and CrCl₃.⁴⁰ Stern-Volmer analysis revealed that the quenching constant of the carboxylate **1a** was substantially greater than that of the other reagents in both CH₃CN and CH₂Cl₂.⁴⁰ This supports a pathway in which the carboxylate substrate **1a** reacts with the excited photocatalyst to undergo oxidative decarboxylation, forming an α -amino radical intermediate **6** (Fig. 4). Consistent with this mechanism, no product formation was observed when either transformation was carried out in the presence of TEMPO (1 equiv.).

Next, to assess the possibility of a radical-radical recombination pathway (not shown), we measured the standard reduction potential ($E_{1/2}$) of 3-oxetanone (**2**) using differential pulse voltammetry (DPV).⁴⁰ We determined an $E_{1/2}$ value of -2.51 V vs. SCE in CH₃CN. In contrast, the redox potentials of 4CzIPN ($E_{1/2}[P^{+}/P^*] = -1.04$ V; $E_{1/2}[P/P^*] = -1.21$ V vs. SCE in CH₃CN)⁴¹ are too small to drive reduction of 3-oxetanone (**2**) to the corresponding ketyl radical. Accordingly, radical-radical recombination pathways were ruled out for both reaction conditions.

In contrast, in the Cr-mediated reaction, the reduction potentials of 4CzIPN^{•-} are sufficient to reduce Cr^{III}L_n to Cr^{II}L_n ($E_{1/2}[\text{Cr}^{\text{III}}/\text{Cr}^{\text{II}}] = -0.51$ V vs. SCE in DMF).⁴² This reduced Cr^{II}L_n can then intercept the α -amino radical **6** to generate alkyl-Cr intermediate **8**, a step that has been extensively investigated in Nozaki-Hiyama-Kishi reaction manifolds,⁴³ which may then add to 3-oxetanone (**2**) to form Cr alkoxide **10**. The reaction may then terminate by protonation to form oxetanol **3a**. Alternatively, it is possible that α -amino radical **6** may undergo direct addition to Brønsted acid-activated 3-oxetanone (**2**) to form radical cation **7**, and there is precedent for such 1,2-additions.^{39,44} Subsequently, photocatalyzed reduction of the radical cation **7** would form oxetanol **3a**, also completing the photocatalytic cycle.

Thus, to investigate these two possibilities, we carried out deuterium quenching experiments using the parent substrate *N*-phenyl glycine (**1a**) with 3-oxetanone (**2**) and/or methanol-*d* (CH₃OD) (Table 3). We anticipated that, in the presence of methanol, the alkyl-Cr intermediate **8**, but not the corresponding α -amino radical species **6**, would be quenched to form the proto(deutero)decarboxylation products **13** (ESI Figure S1†). Under the standard Cr-mediated reaction



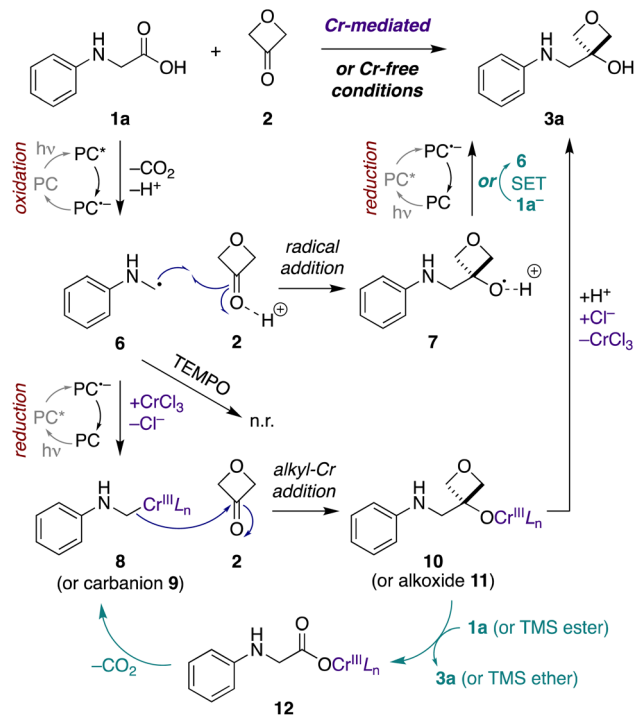


Fig. 4 Possible mechanisms for Cr-mediated and Cr-free photo-redox-catalyzed decarboxylative addition to 3-oxetanone (**2**). Initial photocatalytic oxidative decarboxylation of α -amino acid carboxylate **1a**⁻ forms α -amino radical **6**. Under Cr-mediated conditions (purple), reduction to alkyl-Cr species **8** predominates, with nucleophilic addition to 3-oxetanone (**2**) forming Cr alkoxide **10**. Chain propagation (teal) may occur by conversion of Cr-alkoxide **10** to Cr-carboxylate **12** via either direct proton-Cr exchange or σ -bond metathesis of the corresponding TMS ester of **1a**, followed by decarboxylation to regenerate alkyl-Cr species **8**. Under Cr-free conditions, direct radical addition of α -amino radical **6** to Brønsted-acid activated 3-oxetanone (**2**) predominates, forming radical cation **7**. The reaction may terminate by photocatalyzed reduction of **7** to the product **3a**. Alternatively, chain propagation (teal) may occur through an SET event between **7** and carboxylate **1a**⁻ to furnish the product **3a** and regenerate α -amino radical **6** (teal). A minor pathway in the Cr-mediated reaction may involve this same radical addition (**6** + **2** \rightarrow **7**), while a minor pathway in the Cr-free reaction may involve a free carbanion/alkoxide mechanism (**9** + **2** \rightarrow **11**). *L* = ligand, n.r. = no reaction, PC = photocatalyst, PC* = excited state, PC^{•-} = radical anion state.

conditions, we observed 60% of the 3-oxetanol product **3a** and 14% protodecarboxylation product **13a** (Table 3, entry 1). When 3-oxetanone was omitted and replaced by methanol-*d*, the yield of the proto/deuterodecarboxylation products **13a, b** increased to 59% (combined), with 80% deuterium incorporation (entry 2), consistent with the alkyl-Cr addition pathway. Interestingly, when both 3-oxetanone (**2**) and methanol-*d* were included in the reaction, yields of both the 3-oxetanol product **3a** and the protodecarboxylation products **13a, b** were decreased (entry 3), suggesting that additional undesired reaction pathways become active under these conditions.

In the Cr-free reaction, quenching with methanol-*d* also resulted in formation of the proto/deuterodecarboxylation products **13a, b** (entry 5), consistent with formation of an α -amino carbanion intermediate **9** (Fig. 4 and ESI Figure S1†). In

Table 3 Competition experiments under Cr-mediated and Cr-free reaction conditions

Entry	Conditions ^a	Electrophile	Quencher	3a ^b (%)	13a + 13b (%)
1	Cr-mediated	2 (1 equiv.)	—	60	14
2	Cr-mediated ^c	—	CH ₃ OD	—	59 (80) ^d
3	Cr-mediated ^c	2 (1 equiv.)	CH ₃ OD	48	6 (57) ^d
4	Cr-free	2 (3 equiv.)	—	60	5
5	Cr-free ^c	—	CH ₃ OD	—	47 (55) ^d
6	Cr-free ^c	2 (3 equiv.)	CH ₃ OD	100	—

^a Cr-mediated reaction conditions: 1 mol% 4CzIPN, 5 mol% CrCl₃, 0.5 equiv. TMSCl, 1.2 equiv. CsOPiv, 0.8 M in CH₃CN based on amino acid substrate **1a**, blue LED light, rt, 20 h. Cr-free reaction conditions: 2 mol% 4CzIPN, 1.2 equiv. CsOPiv, 0.5 M in CH₂Cl₂ based on amino acid substrate **1a**, blue LED light, rt, 2 h. ^b Yields based on ¹H-NMR analysis of crude reaction product in the presence of an internal standard, relative to *N*-phenyl glycine (**1a**). ^c Amino acid substrate **1a** was deuterium exchanged with CH₃OD prior to the reaction. ^d Percent deuterium incorporation (**13b**: R = D) shown in parentheses.

contrast, when both 3-oxetanone (**2**) and methanol-*d* were included in the reaction, the yield of the 3-oxetanol product **3a** increased to 100% (entry 6). This is contrary to expectation if the standard Cr-free reaction proceeds solely via a carbanion intermediate. Notably, Glorius and coworkers have proposed that photoredox-initiated intermolecular radical trapping by ketones and aldehydes may be promoted by Brønsted-acid activation of the carbonyl compound.³⁹ Thus, the increased yield observed under these conditions (entries 3 and 6) may be attributed to such activation of 3-oxetanone by methanol. Unfortunately, the improved yield observed in Cr-free reaction in the presence of methanol did not prove generalizable to other *N*-aryl α -amino acid substrates (not shown).

The contrasting results in these competition experiments, in which the reaction conditions are significantly perturbed by omission of the electrophile or addition of a cosolvent, make it difficult to draw definitive conclusions regarding the predominant pathways under the standard Cr-mediated and Cr-free reaction conditions, and suggest that both are possible.

Lastly, we investigated the quantum yields of these transformations. Photon flux of the light source was determined using standard ferrioxalate actinometry.⁴⁰ The quantum yield was then calculated by determining the amount of product formed in 3 min under the standard reaction conditions, and dividing by the photon flux. We observed quantum yields of 5.2 for the Cr-mediated reaction and 10.3 for the Cr-free reaction, indicative of chain propagation mechanisms under both conditions.



In the context of the Cr-mediated reaction, the reduction potentials of carboxylic acid **1a** ($E_{1/2}[\mathbf{1a}^+/\mathbf{1a}] = +0.42$ V vs. SCE in CH_3CN)³⁶ and $\text{Cr}^{\text{III}}\text{L}_n$ ($E_{1/2}[\text{Cr}^{\text{III}}/\text{Cr}^{\text{II}}] = -0.51$ V vs. SCE in DMF)⁴² indicate that direct oxidative decarboxylation of **1a** by $\text{Cr}(\text{III})$ would be thermodynamically unfavorable, making chain propagation *via* a redox mechanism unlikely.

An alternative possibility is that the alkyl-Cr species **8** is regenerated *via* a cycle in which the Cr-alkoxide intermediate **10** reacts with a new equivalent of the carboxylic acid substrate **1a** to form Cr-carboxylate **12**, which then undergoes metal-mediated decarboxylation to form alkyl-Cr species **8**.^{45,46} Formation of Cr-carboxylate **12** could occur either *via* direct proton-Cr exchange with carboxylic acid **1a**, or *via* σ -bond metathesis with the corresponding TMS ester, as postulated by Glorius and coworkers in related propagation reactions with trimethylsilylmethylamines,¹⁵ with subsequent desilylation of the resultant TMS ether to the product **3a**. Consistent with the latter hypothesis, when TMSCl was omitted from the reaction, the quantum yield dropped to 1.6, indicating an important role in the propagation cycle.

In the Cr-free reaction, chain propagation may occur *via* SET between radical cation **7** and carboxylate $\mathbf{1a}^-$ ($E_{1/2}[\mathbf{1a}^+/\mathbf{1a}^-] = +0.42$ V vs. SCE in CH_3CN)³⁶ to regenerate α -amino radical **6** and furnish 3-oxetanone product **3a**. This electron transfer event should be thermodynamically favorable, based on the computationally determined redox potential of an alkoxy radical cation-to-alcohol conversion by Glorius and coworkers.³⁹

Taken together, these results suggest that Cr-mediated reaction proceeds predominantly *via* the alkyl-Cr addition pathway (**8** + **2** → **10**), because omission of TMSCl results in a large decrease in quantum yield (5.2 to 1.6), indicating the importance of the Cr-based chain propagation cycle (**10** → **12** → **8**) compared to the SET chain propagation cycle (**7** → **6**) (ESI Fig. S2†). In contrast, the Cr-free reaction cannot involve the Cr-based chain propagation cycle (and the free carboxylate analogue of **12** would not decarboxylate spontaneously to form carbanion **9**). Thus, the high quantum yield in that reaction (10.3) must be attributed to the SET propagation cycle, which can only arise from the radical addition pathway (**6** + **2** → **7**). Thus, while both reaction manifolds may be operative to some extent under both conditions, it appears that the Cr-mediated reaction proceeds mainly *via* the alkyl-Cr pathway and the Cr-free reaction proceeds mainly *via* the radical addition pathway.

Conclusions

In summary, by leveraging photoredox catalysis, we have successfully developed a method for direct conversion of α -amino acids to bioisosteric 3-oxetanones, thus avoiding the lengthy *de novo* synthesis approaches that have been used previously to access such motifs. Mechanistic investigations support a pathway involving initial oxidative decarboxylation to an α -amino radical species, which can then undergo direct radical addition to 3-oxetanone, or intermediate reduction to an α -amino alkyl-Cr or carbanion species followed by nucleophilic addition to 3-oxetanone, with the dominant reaction manifold dictated by the presence or absence of Cr. Notably, in both cases,

chain propagation provides quantum yields >5. This methodology is applicable to a wide range of *N*-aryl α -amino acids, a motif which has been reported to have a variety of potential therapeutic applications in infectious disease, inflammation, neurodegeneration, and metabolic and gastrointestinal diseases.^{47–49} The substrate scope of the Cr-free reaction also includes *N,N*-dialkyl α -amino acid substrates. Efforts to expand the substrate scope further to other carboxylic acids are under active investigation in our lab. This direct conversion of carboxylic acids to 3-oxetanones should facilitate further investigation of these attractive bioisosteres in medicinal chemistry.

Author contributions

A. M. V. D. R., C. S. N. E., A. M., and D. S. T. conceptualized the experiments; A. M. V. D. R. and C. S. N. E. performed the experiments with assistance from M. I. H.; A. M. V. D. R. and D. S. T. prepared the manuscript; A. M. V. D. R., C. S. N. E., A. M., and D. S. T. edited the manuscript.

Conflicts of interest

There are no conflicts to declare.

Acknowledgements

We thank Prof. Tomislav Rovis (Columbia University), Prof. Tehshik Yoon and Dr Wesley Swords (University of Wisconsin-Madison), and Prof. Uttam Tambar (University of Texas, Southwestern Medical Center) for helpful discussions, Dr George Sukenick and Rong Wang (MSK Analytical NMR Core Facility) for expert NMR and mass spectral support, and Prof. Jonathan Goldberg (MSK) and Prof. Jason Lewis (MSK) for generous assistance with instrumentation. Financial support from the NIH (T32 CA062948-Gudas to A. M. V. D. R., T32 GM136640-Tan to C. S. N. E., and CCSG P30 CA008748 to S. M. Vickers) and MSK Basic Research Initiative (to A. M. V. D. R., A. M., and D. S. T.) is gratefully acknowledged.

Notes and references

- 1 F. Mao, W. Ni, X. Xu, H. Wang, J. Wang, M. Ji and J. Li, *Molecules*, 2016, **21**, 1–18.
- 2 J. Ghuman, P. A. Zunszain, I. Petitpas, A. A. Bhattacharya, M. Otagiri and S. Curry, *J. Mol. Biol.*, 2005, **353**, 38–52.
- 3 C. Skonberg, J. Olsen, K. G. Madsen, S. H. Hansen and M. P. Grillo, *Expert Opin. Drug Metab. Toxicol.*, 2008, **4**, 425–438.
- 4 A. Kalgutkar and J. Daniels, *RSC Drug Discovery Ser.*, 2010, **1**, 99–167.
- 5 C. Ballatore, D. M. Huryn and A. B. Smith III, *ChemMedChem*, 2013, **8**, 385–395.
- 6 P. S. Charifson and W. P. Walters, *J. Med. Chem.*, 2014, **57**, 9701–9717.
- 7 M. V. Varma, B. Feng, R. S. Obach, M. D. Troutman, J. Chupka, H. R. Miller and A. El-Kattan, *J. Med. Chem.*, 2009, **52**, 4844–4852.



- 8 Z. P. Qureshi, E. Seoane-Vazquez, R. Rodriguez-Monguio, K. B. Stevenson and S. L. Szeinbach, *Pharmacoepidemiol. Drug Saf.*, 2011, **20**, 772–777.
- 9 N. Brown, in *Bioisosteres in Medicinal Chemistry*, 2012, pp. 1–14.
- 10 P. Lassalas, K. Oukoloff, V. Makani, M. James, V. Tran, Y. Yao, L. Huang, K. Vijayendran, L. Monti, J. Q. Trojanowski, V. M. Y. Lee, M. C. Kozlowski, A. B. Smith, K. R. Brunden and C. Ballatore, *Med. Chem. Lett.*, 2017, **8**, 864–868.
- 11 T. Bach, K. Jödicke, K. Kather and R. Fröhlich, *J. Am. Chem. Soc.*, 1997, **119**, 2437–2445.
- 12 D. R. Witty, G. W. J. Fleet, K. Vogt, F. X. Wilson, Y. Wang, R. Storer, P. L. Myers and C. J. Wallis, *Tetrahedron Lett.*, 1990, **31**, 4787–4790.
- 13 J. A. Bull, R. A. Croft, O. A. Davis, R. Doran and K. F. Morgan, *Chem. Rev.*, 2016, **116**, 12150–12233.
- 14 K. Donabauer, M. Maity, A. L. Berger, G. S. Huff, S. Crespi and B. König, *Chem. Sci.*, 2019, **10**, 5162–5166.
- 15 J. L. Schwarz, R. Kleinmans, T. O. Paulisch and F. Glorius, *J. Am. Chem. Soc.*, 2020, **142**, 2168–2174.
- 16 G. Wuitschik, M. Rogers-Evans, K. Muller, H. Fischer, B. Wagner, F. Schuler, L. Polonchuk and E. M. Carreira, *Angew. Chem., Int. Ed.*, 2006, **45**, 7736–7739.
- 17 G. Wuitschik, E. M. Carreira, B. Wagner, H. Fischer, I. Parrilla, F. Schuler, M. Rogers-Evans and K. Muller, *J. Med. Chem.*, 2010, **53**, 3227–3246.
- 18 J. A. Burkhard, G. Wuitschik, M. Rogers-Evans, K. Muller and E. M. Carreira, *Angew. Chem. Int. Ed. Engl.*, 2010, **49**, 9052–9067.
- 19 M. Rogers-Evans, H. Knust, J.-M. Plancher, E. M. Carreira, G. Wuitschik, J. Burkhard, D. B. Li and C. Guérot, *Chimia*, 2014, **68**, 492–499.
- 20 M. McLaughlin, R. Yazaki, T. C. Fessard and E. M. Carreira, *Org. Lett.*, 2014, **16**, 4070–4073.
- 21 G. P. Möller, S. Müller, B. T. Wolfstädter, S. Wolfrum, D. Schepmann, B. Wunsch and E. M. Carreira, *Org. Lett.*, 2017, **19**, 2510–2513.
- 22 J. A. Burkhard, G. Wuitschik, J.-M. Plancher, M. Rogers-Evans and E. M. Carreira, *Org. Lett.*, 2013, **15**, 4312–4315.
- 23 S. Roesner, J. D. Beadle, L. K. B. Tam, I. Wilkening, G. J. Clarkson, P. Raubo and M. Shipman, *Org. Biomol. Chem.*, 2020, **18**, 5400–5405.
- 24 M. H. Shaw, J. Twilton and D. W. C. MacMillan, *J. Org. Chem.*, 2016, **81**, 6898–6926.
- 25 R. C. McAtee, E. J. McClain and C. R. J. Stephenson, *Trends Chem.*, 2019, **1**, 111–125.
- 26 A. Gil, F. Albericio and M. Álvarez, *Chem. Rev.*, 2017, **117**, 8420–8446.
- 27 D. R. G. Brimage, R. S. Davidson and P. R. Steiner, *J. Chem. Soc., Perkin Trans.*, 1973, **1**, 526–529.
- 28 Z. Su, P. S. Mariano, D. E. Falvey, U. C. Yoon and S. W. Oh, *J. Am. Chem. Soc.*, 1998, **120**, 10676–10686.
- 29 Z. Zuo, D. T. Ahneman, L. Chu, J. A. Terrett, A. G. Doyle and D. W. C. MacMillan, *Science*, 2014, **345**, 437–440.
- 30 Z. Zuo and D. W. C. MacMillan, *J. Am. Chem. Soc.*, 2014, **136**, 5257–5260.
- 31 L. Chu, C. Ohta, Z. Zuo and D. W. C. MacMillan, *J. Am. Chem. Soc.*, 2014, **136**, 10886–10889.
- 32 K. Nakajima, Y. Miyake and Y. Nishibayashi, *Acc. Chem. Res.*, 2016, **49**, 1946–1956.
- 33 A. Millet, Q. Lefebvre and M. Rueping, *Chem.–Eur. J.*, 2016, **22**, 13464–13468.
- 34 S. Pan, M. Jiang, J. Hu, R. Xu, X. Zeng and G. Zhong, *Green Chem.*, 2020, **22**, 336–341.
- 35 H. Wen, R. Ge, Y. Qu, J. Sun, X. Shi, W. Cui, H. Yan, Q. Zhang, Y. An, W. Su, H. Yang, L. Kuai, A. L. Satz and X. Peng, *Org. Lett.*, 2020, **22**, 9484–9489.
- 36 H. Peng, S. Bi, M. Ni, X. Xie, Y. Liao, X. Zhou, Z. Xue, J. Zhu, Y. Wei, C. N. Bowman and Y.-W. Mai, *J. Am. Chem. Soc.*, 2014, **136**, 8855–8858.
- 37 A. Noble and D. W. C. MacMillan, *J. Am. Chem. Soc.*, 2014, **136**, 11602–11605.
- 38 A. Fürstner and N. Shi, *J. Am. Chem. Soc.*, 1996, **118**, 2533–2534.
- 39 L. Pitzer, F. Sandfort, F. Strieth-Kalthoff and F. Glorius, *J. Am. Chem. Soc.*, 2017, **139**, 13652–13655.
- 40 See ESI† for complete details.
- 41 J. Luo and J. Zhang, *ACS Catal.*, 2016, **6**, 873–877.
- 42 K. Izutsu, in *Electrochemistry in Nonaqueous Solutions*, Wiley-VCH, 2009, pp. 89–110.
- 43 Y. Katayama, H. Mitsunuma and M. Kanai, *Synthesis*, 2022, **54**, 1684–1694.
- 44 H.-M. Huang, P. Bellotti and F. Glorius, *Acc. Chem. Res.*, 2022, **55**, 1135–1147.
- 45 T. Galcera, X. Jouan and M. Bolte, *J. Photochem. Photobiol., A*, 1988, **45**, 249–259.
- 46 G. B. Deacon, S. J. Faulks and G. N. Pain, in *Advances in Organometallic Chemistry*, ed. F. G. A. Stone and R. West, Academic Press, 1986, vol. 25, pp. 237–276.
- 47 N. B. Tien, N. P. Buu-Hoï and N. D. Xuong, *J. Org. Chem.*, 1958, **23**, 186–188.
- 48 D. Schuster, M. Zederbauer, T. Langer, A. Kubin and P. G. Furtmüller, *J. Enzyme Inhib. Med. Chem.*, 2018, **33**, 1529–1536.
- 49 N. Tanaka, T. Tamai, H. Mukaiyama, A. Hirabayashi, H. Muranaka, S. Akahane, H. Miyata and M. Akahane, *J. Enzyme Inhib. Med. Chem.*, 2001, **44**, 1436–1445.

